

# Research on selected location algorithms for the unmanned ground vehicles operating in a follow-me scenario based on ultra-wideband positioning system

Łukasz Rykała<sup>1\*</sup> , Mirosław Przybysz<sup>1</sup> , Karol Cieślak<sup>1</sup> , Piotr Krogul<sup>1</sup> ,  
Rafał Typiak<sup>1</sup> , Andrzej Typiak<sup>1</sup> 

<sup>1</sup> Faculty of Mechanical Engineering, Military University of Technology, ul. gen. Sylwestra Kaliskiego 2, 00-908 Warsaw, Poland

\* Corresponding author's e-mail: lukasz.rykala@wat.edu.pl

## ABSTRACT

Ultra wideband (UWB) technology is a highly developed wireless radio communication technology used, among others, in location systems. The article focused on using UWB technology to construct a guide location system for an unmanned ground vehicle (UGV). In order to carry out the research, the parameters of the measurement noise occurring in real UWB modules were determined. The mentioned noise simulated disturbed distance measurement indications, modelling real measurements. The paper presented the results of simulation research of selected location algorithms for a guide location system based on UWB technology. The work compared the total location errors of the guide of selected algorithms based on geometric methods, trilateration and optimisation methods. Simulation studies allow for quick testing of algorithms, taking into account real disturbances and constitute the first stage of work on implementing various algorithms in a real positioning system. The most accurate in the context of guide location among the analysed algorithms was the Levenberg–Marquardt algorithm (lowest value of the average quality index). The geometric method, due to the least complex mathematical model and high susceptibility to interference, was in turn the least accurate location algorithm among the analysed ones.

**Keywords:** UGV, follow-me, ultra-wideband, positioning system, location algorithms.

## INTRODUCTION

Unmanned ground vehicles are land robots that move without a human being on board [1]. They have found application in many areas, both military and civilian, where human presence would be difficult or even pose a threat to his life. In the military field, UGVs are used, among others, to transport supplies, ammunition, and other materials to the battlefield, conduct reconnaissance missions, collect information without endangering the health of soldiers or evacuate the wounded from the battlefield [1–4]. In turn, in the civil field of UGV, there are, among others: used in rescue operations, e.g. during disasters, to automate logistics processes, i.e. transport of materials in warehouses and factories, in agriculture,

where they are used to monitor crops, apply pesticides, and harvest [5–7]. UGVs can operate under difficult conditions and thus contribute to increasing the efficiency and safety of various activities, both hazardous to people but also during the automation of repetitive, simple activities. In the context of UGVs, two key problems should be distinguished, i.e. navigation and control. which are complex issues including, among others: determining the current position of the vehicle (location), determining the movement trajectory and its implementation [8].

Some of the UGVs can operate fully autonomously. Autonomous operation means that the vehicle can move independently in its working environment using a set of sensors designed for this purpose [9]. The mentioned operating mode

is not the only one used in UGVs, which can also be controlled remotely or using teleoperation [10]. In the case of remotely controlled vehicles, the operator has full control over the vehicle, observes its operation and surroundings from a safe distance, and controls its systems using the controller [10]. In turn, teleoperated UGVs are an extension of the functionality of remotely controlled vehicles. In the case of autonomous UGVs, the operator's role is only to supervise the implementation of tasks. Autonomous vehicles are equipped with several sensors that enable them to observe the surroundings and locate in the field [11–12].

An additional group of UGVs are following vehicles, which have the functionality of following a guide (so-called follow me) [13–14]. When moving, the guide (operator, vehicle) indicates the route to the machine following him. The advantage of this solution is that the operator does not have to manually control the vehicle, which follows the guide using signals from a sensor or set of sensors mounted on it [10, 13–14]. The solutions discussed complement the basic functionality of teleoperated ground vehicles. Working in this mode UGV follows the guide using on-board observation systems. In the guide-following mode, the movement path of a UGV is generated based on the designated position of the guide, which is within the range of observation sensors installed on the vehicle. The operator follows the guide, while the vehicle steering system recreates its path, with an assumed delay (without any necessary actions on the part of the operator), considering the dimensions of the vehicle and maintaining a safe distance to the guide [15–17].

The main task of the guide is to follow the route passable by the vehicle. The tasks of the onboard control system are to identify the guide, determine its route, locate other objects in the vicinity of the vehicle and steer the machine along the designated route. The implementation of these functionalities is ensured by the guide following system, which includes the following subsystems: guide location, guide route determination, environmental observation, navigation, and control. The guide localisation subsystem is a key component of guide following systems [17–18]. It ensures the determination of the position of a moving guide. Its essence can be implemented based on various technologies, ranging from vision, laser, and ultrasonic systems to wireless communication systems. Technologies for observing humans and their surroundings are the basis for the functioning of guide following

systems [17]. Ultra-Wideband (UWB) technology is an often used solution for vehicle localisation [19–21] and guide-following applications [22–23], offering real-time localisation with centimeter-level precision [24]. It is known for its low energy consumption, interference immunity (minimally affecting existing radio systems), and high resilience to multipath signal effects in both line of sight (LOS) and non-line of sight (NLOS) scenarios [25–26]. However, UWB systems have some limitations, including a restricted range due to their low-power and dependence on the surroundings [27]. Additionally, the proximity of UWB devices to the human body can negatively impact their accuracy and operational range [28].

The aim of the article paper was to determine the guide localisation errors for selected localisation algorithms, taking into account the actual noise in UWB measurements. Simulation studies of the guide localisation system were focused on the selection of a localisation algorithm characterised by minimal localisation errors. The article was organised into 5 parts: introduction, materials and methods, results, discussion, and conclusions.

## **MATERIALS AND METHODS**

### **Preliminary experimental research**

The key task enabling the realisation of simulation studies is to determine the measurement noise parameters simulating the actual disturbances affecting the UWB modules. A Decawave TREK1000 set [29], which consists of five UWB modules, was used in the conducted research. The developed system consists of four anchors and one tag that perform continuous distance measurements.

UWB modules were deployed on the vehicle (anchors) and the guide (tag). The system provides information about the distance from individual anchors to the tag. On their basis, it is possible to determine the position of the guide relative to the coordinate system associated with the UGV. The measured value is given in millimetres and updated at a frequency of 10 Hz. The refresh rate depends on the configuration of the module's operating band, which can be set in the range from 3.5 to 6.5 GHz [17]. UWB modules use a two-way ranging method called two way ranging (TWR) [30], a variation of the time of arrival (TOA) method. In order to compare the simulation and experimental results, the total

location errors were determined using geometric methods. The UGV “Dromader” was adopted for the research. Four anchors of the UWB system: K1, K2, K3, K4 were mounted on the UGV (Figure 1), and the tag was mounted on a tripod.

Anchors K1, K2, K3 and K4 were mounted on the UGV in a configuration that ensured direct visibility between the tag and each of the anchors. It was assumed that the research would involve 80 measurement series with a duration of 45 s, consisting of placing a stationary tag at previously determined measurement points. For the research, the x-y coordinate system was adopted, which was associated with the stationary UGV [31]. In turn, Figure 2 shows a diagram of the arrangement of 80

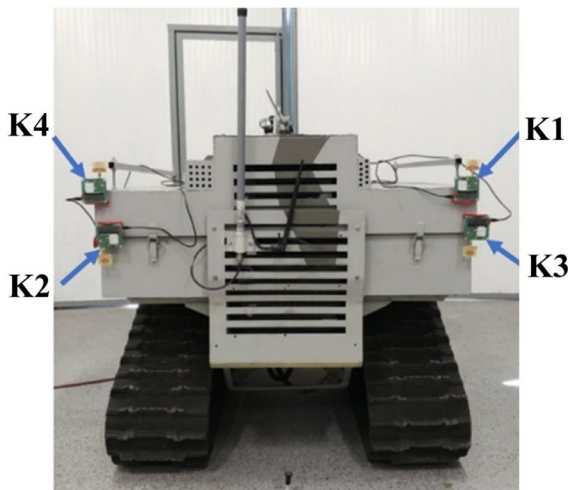


Figure 1. Selected UGV with anchors K1, K2, K3, K4. Own elaboration based on [10]

measurement points P1 – P80, spaced 0.5 m apart, where distance measurements were conducted.

In the case of simulation studies, for each of the points, the  $x_G(t)$ ,  $y_G(t)$  projections of the guide position on the x, y axes of the coordinate system associated with the UGV were generated. Then, knowing the location of the anchors and the  $x_G(t)$ ,  $y_G(t)$ , the theoretical distances from the anchors were determined:

$$d_{t1} = \sqrt{(x_G - x_1)^2 + (y_G - y_1)^2} \quad (1)$$

$$d_{t2} = \sqrt{(x_G - x_2)^2 + (y_G - y_2)^2} \quad (2)$$

$$d_{t3} = \sqrt{(x_G - x_3)^2 + (y_G - y_3)^2} \quad (3)$$

$$d_{t4} = \sqrt{(x_G - x_4)^2 + (y_G - y_4)^2} \quad (4)$$

In order to obtain distance courses simulating the actual readings of UWB modules, the following relationship was used:

$$d_{si} = d_{ti} + z_i \quad (5)$$

where:  $d_{si}$  – the simulated distance between i-th anchor  $K_i$  ( $i = 0, 1, 2, 3$ ) and the tag,  $d_{ti}$  – the distance between i-th anchor  $K_i$  ( $i = 0, 1, 2, 3$ ) and tag determined with the use of (1), (2), (3), (4),  $z_i$  – disturbance of the i-th anchor measurement  $K_i$  ( $i = 0, 1, 2, 3$ ).

On the basis of the manufacturer’s documentation of the UWB module, the maximum error of distance measurements in the TREK1000 set is 0.1 m [29]. On this basis, it was assumed that the disturbances in anchor distance measurements  $z_i$  ( $i = 0, 1, 2, 3, 4$ ) are characterised by

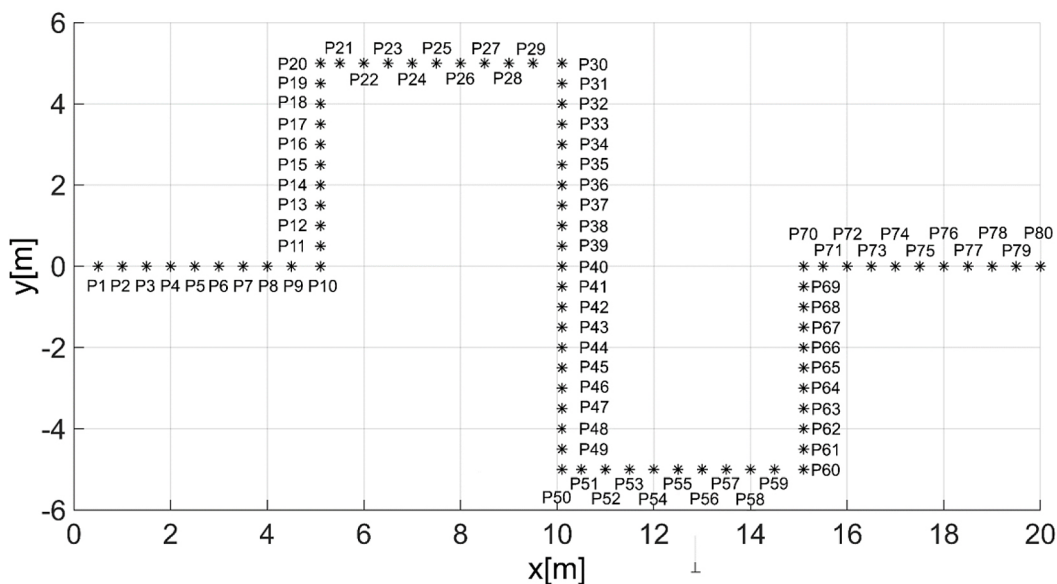


Figure 2. Diagram of the arrangement of measurement points P1 – P80 [23]

a standard deviation of 0.02 m and is generated independently for each anchor. Moreover, it was assumed that the disturbance was characterised by a normal distribution. The distances determined during the simulation were statistically modelled without analysing the impact of the vehicle and module assembly.

Determining the location of the tag (in the x-y coordinate system) is possible using measurements from pairs of anchors lying on opposite sides of the UGV: (1,2), (1,4), (3,2), (3,4). In this way, a total of four label locations are obtained: K12, K14, K32, and K34, the final location of which can be determined using the arithmetic mean:  $K_{av}$ .

Then, the marginal positions P10, P20, P30, P40, P50, P60, P70, P80 were selected for

further research. On the basis of the indications from the modules, the values of the average total errors  $e_{av}$  were determined for the mentioned measurement points.

During the experimental research, proprietary software for receiving data from UWB modules made in Matlab/Simulink was used. Moreover, Figure 3 shows the results of the average total error for selected measurement points. The analysis of the obtained experimental test results (Figure 3) shows that the average total location error in determining the position of the guide at a distance of 5 m from the UGV (P10) does not exceed 0.13 m, at a distance of 10 m from the UGV (P40) does not exceed 0.24 m, while at a distance of 20 m from UGV (P80) it is no more than 0.48 m.

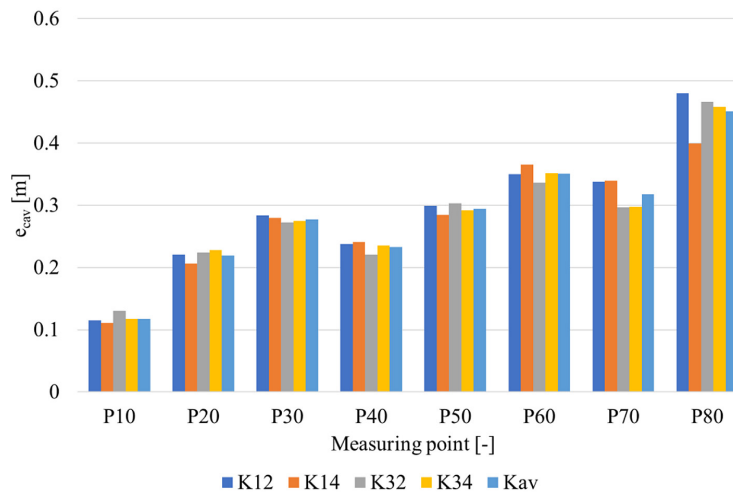


Figure 3. Values of average total errors  $e_{av}$  for selected measurement points in the case of experimental studies. Own elaboration based on [10]

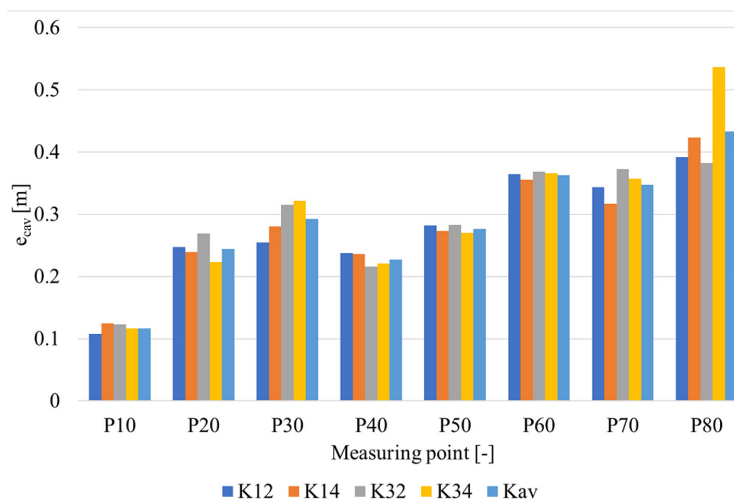


Figure 4. Values of average total errors  $e_{av}$  for selected measurement points in the case of simulation studies. Own elaboration based on [10]

The analysis of the obtained simulation results (Figure 4) shows that the average total error in determining the position of the guide at a distance of 5 m from the UGV (P10) does not exceed 0.13 m, at a distance of 10 m from the UGV (P40) does not exceed 0.24 m, while at a distance of 20 m from UGV (P80) it is no more than 0.54 m.

Figure 5 shows a comparison between the results of simulation tests with the results of experimental tests for analogous measurement points in the case of averaged positions from all anchors - Kav. The next step was to determine the  $\Delta e$  parameter value, which is the absolute difference between the simulation and experimental values (Figure 6) obtained according to the following relationship:

$$\Delta e = |e_{cav_{sim}} - e_{cav_{exp}}| \quad (6)$$

The analysis of the results obtained (Figure 6) for both tests shows minor differences between the simulation and experimental results (max. difference value approx. 0.03 m). The tests of the localisation subsystem showed small values of total errors in the results of simulation and experimental tests (Figure 5), which allows concluding that the generated disturbance waveforms in the case of simulation tests, i.e. a normal distribution with a standard deviation of 0.02 m, reflect the real noises that are properties of the measurement systems in UWB modules [10].

As a result, the research showed that the total location errors also increase along with the distance between the guide and the UGV due to the limited accuracy of UWB module measurements.

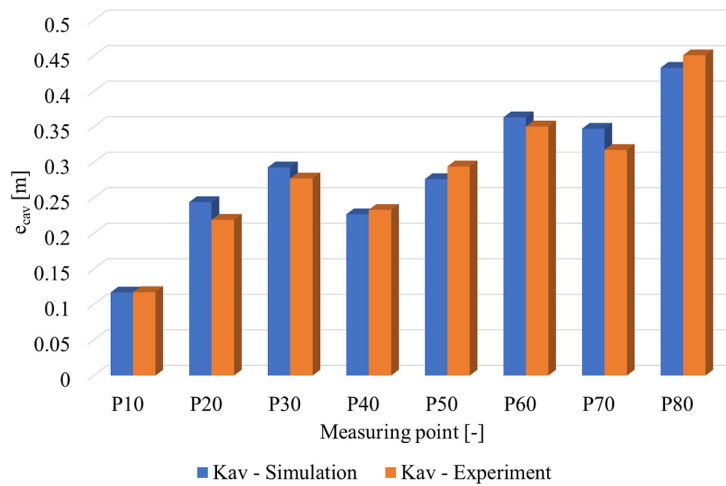


Figure 5. Summary of the results of simulation and experimental tests for selected measurement points. Own elaboration based on [10]

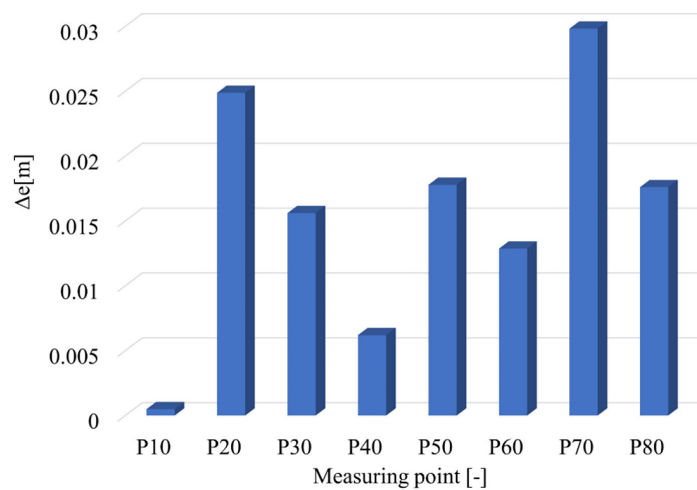


Figure 6. Summary of the results of the absolute value of the difference in total errors of simulation and experimental tests for selected measurement points. Own elaboration based on [10]

### Simulation research

The basis for determining the mathematical model of selected location algorithms is to determine the basic geometric relationships necessary to process distance measurements from the UWB modules. After placing the anchors on the vehicle, their location should be described in the selected coordinate system. For this purpose, it was assumed that all anchors ( $A_1, A_2, A_3, A_4$ ) are located on the UGV, and their configuration is shown in Figure 7. In turn, the tag is attached to the moving guide. The tag and anchors are positioned as described in the cartesian coordinate system  $xyz$  at the following points: guide  $G (x_G, y_G, z_G)$ ; anchor no. 1:  $A_1 (x_1, y_1, z_1)$ ; anchor no. 2:  $A_2 (x_2, y_2, z_2)$ ; anchor no. 3:  $A_3 (x_3, y_3, z_3)$ ; anchor no. 4:  $A_4 (x_4, y_4, z_4)$ . Relationships (1), (2), (3), and (4) describe elementary geometric relationships between the position of the guide (point  $G$ ) and the position of anchors (points  $A_1, A_2, A_3, A_4$ ) in the two-dimensional  $x$ - $y$  coordinate system.

### Selected location algorithms

Various positioning algorithms are used for UWB positioning, including the Kalman filter [32–33], trilateration [34–37], genetic algorithms [38], fuzzy logic [39, 40], optimisation methods [17, 38], hybrid methods [41], etc. Three characteristic methods for determining the location of

the guide were selected in the work: trilateration, geometric methods, and the Levenberg-Marquardt algorithm. The most frequently used solution in UWB positioning systems is trilateration due to the linear relationship between the input signals ( $d_1, d_2, d_3, d_4$ ) and the searched guide location ( $x_G, y_G$ ). A solution that does not require linearisation, but is much less computationally complex, is geometric methods that use only two equations to determine the location of the guide [31]. As in the case of trilateration, geometric methods determine the location directly from the dependencies implemented in the method [17]. In turn, the most computationally complex algorithms use optimisation methods to determine the location that minimises the objective function, which requires several iterations. One of the optimisation methods widely used in practice is the Levenberg–Marquardt algorithm due to the robustness, efficiency, and flexibility of the solution [10]. Localisation algorithms are also of great importance in the context of many transportation problems [42–43].

The selected methods constitute three separate approaches to solving the problem of guide location, selected based on the analysis of existing solutions. Further, the following abbreviations were adopted to describe the mentioned methods: geometric methods (GEO), trilateration (TRI), and Levenberg-Marquardt algorithm (LM).



Figure 7. Anchor configuration on the UGV. Own elaboration based on [10]

### Geometric method

The geometric method (GEO) relies on the fact that the relationships (1), (2), (3), and (4) are quadratic equations with two variables ( $x_G, y_G$ ), enabling the determination of the guide's position using just two selected equations. It is also necessary to assume that the guide is always positioned ahead of the UGV. Not all pairs of anchors are suitable for determining the guide's location. This can be achieved using anchor pairs: (1,3), (1,4), (2,3), and (2,4), which are situated on opposite sides of the UGV. However, using anchor pairs (1,2) and (3,4) leads to significant numerical errors due to the anchors being positioned too close. The position of the guide can be determined from four pairs of anchors: (1,3), (1,4), (2,3) and (2,4), where the arithmetic mean is the final position of the guide  $[x_L, y_L]^T$ :

$$x_G = \frac{x_{G13} + x_{G14} + x_{G23} + x_{G24}}{4} \quad (7)$$

$$y_G = \frac{y_{G13} + y_{G14} + y_{G23} + y_{G24}}{4} \quad (8)$$

where:  $[x_{Gij}, y_{Gij}]^T$  – the position of the guide determined by the pair of  $(i, j)$  anchors.

### Trilateration

Trilateration (TRI) is a fundamental algorithm used in UWB positioning. Dependencies (1), (2), (3), and (4) are non-linear equations due to the unknowns ( $x_G, y_G$ ), which makes it difficult to directly determine the position of the guide. In the case of the discussed dependencies, the use of simple analytical transformations leads to a linear system of equations in closed form. For this purpose, a reference anchor needs to be adopted. The following differences between the reference anchor (anchor no. 1) and the rest of the anchors are then determined:

$$d_{t1}^2 - d_{tj}^2 = 2x_G(x_j - x_1) + 2y_G(y_j - y_1) + k_1 - k_j \quad (9)$$

where:  $k_j = x_j^2 + y_j^2, j = 2, 3, 4$ .

In the 2D case under consideration, in which the number of anchors  $n = 4$ , the guide position can be determined using the least squares method:

$$X_T = (A^T A)^{-1} A^T Y \quad (10)$$

where:

$$Y = \begin{bmatrix} d_{s1}^2 - d_{s2}^2 - k_1 + k_2 \\ d_{s1}^2 - d_{s3}^2 - k_1 + k_3 \\ d_{s1}^2 - d_{s4}^2 - k_1 + k_4 \end{bmatrix} \quad (11)$$

$$A = \begin{bmatrix} 2(x_2 - x_1) & 2(y_2 - y_1) \\ 2(x_3 - x_1) & 2(y_3 - y_1) \\ 2(x_4 - x_1) & 2(y_4 - y_1) \end{bmatrix} \quad (12)$$

$$X_T = \begin{bmatrix} x_G \\ y_G \end{bmatrix} \quad (13)$$

The mathematical model of the trilateration (9) uses simulated distance values  $d_{si}$  ( $i = 1, 2, 3, 4$ ) to take into account the influence of disturbance on the localisation results.

### Levenberg–Marquardt algorithm

The Levenberg–Marquardt (LM) algorithm is an optimisation technique that combines the concepts of the Gradient Descent (GD) and the Gauss-Newton (GN) methods. It is particularly effective for solving non-linear least squares problems, which are common in UWB positioning. The problem of determining guide location can be presented as follows: a system of four non-linear dependencies  $G_i(x)$  ( $i = 1, 2, 3, 4$ ) is given:

$$G_1(x) = \sqrt{(x_G - x_1)^2 + (y_G - y_1)^2} - d_{s1} \quad (14)$$

$$G_2(x) = \sqrt{(x_G - x_2)^2 + (y_G - y_2)^2} - d_{s2} \quad (15)$$

$$G_3(x) = \sqrt{(x_G - x_3)^2 + (y_G - y_3)^2} - d_{s3} \quad (16)$$

$$G_4(x) = \sqrt{(x_G - x_4)^2 + (y_G - y_4)^2} - d_{s4} \quad (17)$$

It is an iterative algorithm, which starts with an initial guess  $x_0 = [x_o, y_o]^T$  for the parameters. It aims to iteratively solve a set of equations  $G_i(x) = 0$  ( $i = 1, 2, 3, 4$ ) by minimising the cost function  $g(x)$  defined as follows:

$$\min_x g(x) = G_1(x)^2 + G_2(x)^2 + G_3(x)^2 + G_4(x)^2 \quad (18)$$

The algorithm calculates iteratively the Jacobian matrix  $J(x_k)$ , which is used to determine the direction and magnitude of the parameter updates  $d_k$ , guided by a damping factor  $\mu_k$  that controls the process according to the following relationship:

$$(J(x_k)^T J(x_k) + \mu_k I) d_k = -J(x_k)^T G(x_k) \quad (19)$$

where:  $J(x_k)$  – Jacobian matrix of  $G(x_k)$ , at iteration  $k$ ,  $d_k$  – search direction vector,  $\mu_k$  – scalar damping parameter.

The described method achieves a compromise between GD and GN. It functions according to the GD when the solution is far from the initial guess, which ensures stability and convergence of the process. In turn, it switches to the GN, when the

solution gets closer to the estimate, taking advantage of the quick rate of convergence.

### Description of simulation research

The simulation studies carried out consider a scenario in which the guide moves along seven rectilinear motion paths set at a specific angle in relation to the x-axis of the x-y coordinate system. It was assumed that the angles mentioned are 0°, 30°, 60°, 90°, 120°, 150° and 180°. The described movement takes place in a limited space of 400 m<sup>2</sup> (-10 m < x < 10 m, 0 m < y < 20 m), as shown graphically in Figure 8.

The choice of the 2D system was due to the fact that in the case of the guide-following system on the flat terrain, vertical movement of the transmitter (z-axis) is negligible. During the movement of the guide, the UGV remains stationary, while the arrangement of anchors is consistent with the configuration shown in Figure 7. Nevertheless, the proposed configuration of the anchor arrangement allows for 3D localisation. In further studies, however, the variant with the 2D system was selected, which is the basis for later path determination and movement planning.

In real UWB systems, the anchor positions must meet a number of assumptions regarding their spatial arrangement. In the case of a 2D system, they should be spaced as far apart as possible, which guarantees greater receiver-transmitter visibility, while the necessary condition for their proper arrangement in 2D is that it is impossible to draw a straight line through which the anchor positions pass. Otherwise, localisation in this case is impossible. Similarly, in the case of the 3D system, where the anchor positions cannot be located on the same plane.

The movement of the guide in the UGV operating area causes a change in the indications of simulated distance measurements observed from individual anchors. In order to reflect real measurements, the simulated anchor distance values were disturbed with normally distributed noise and a standard deviation of 0.02 m. The mentioned parameters were determined based on the test results described in the subsection regarding noise parameters of the location system. In turn, in order to determine the impact of the tested algorithms on the localisation results, the signal filtering process was omitted. Additionally, it was assumed that there were no data packet losses (no signal loss), the presence of a condition of direct visibility of modules (LOS) and the module sampling frequency of 10 Hz (value of the sampling frequency of the UWB modules of the TREK1000 set) [10].

In the next stage, the locations of the guide were determined using three previously selected and described algorithms: GEO, TRI, and LM. In order to evaluate the localisation results, the following values were determined:

- total location error:

$$e_T(t) = \sqrt{(x_z(t) - x_G(t))^2 + (y_z(t) - y_G(t))^2} \quad (20)$$

where:  $x_z(t)$ ,  $y_z(t)$  – values of the assumed x and y coordinates of the guide, at time t,  $x_G(t)$ ,  $y_G(t)$  – the values of the x, and y coordinates of the guide determined using localisation algorithms, at time t.

- quality indicator:

$$Q = \sum e_T(t) \quad (21)$$

where: Q – quality indicator [17].

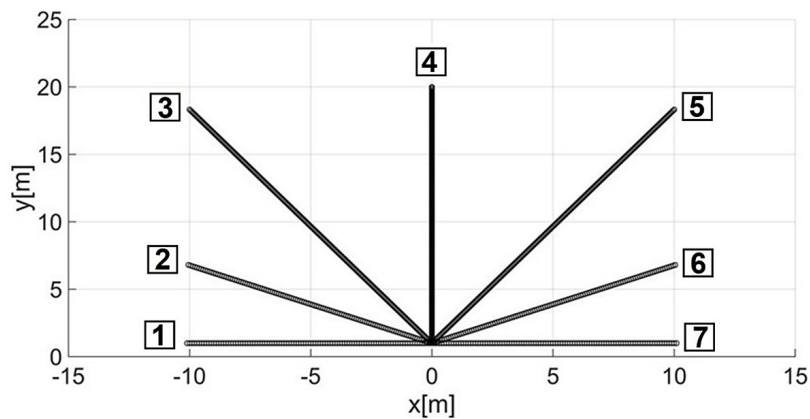


Figure 8. Generated guide location for paths 1–7

- average value of the quality indicator:

$$Q_{av} = \frac{\sum e_T(t)}{n} \quad (22)$$

where:  $n$  – number of distance measurements for individual paths [17].

The evaluation of the results of simulation studies is based on indicators regarding total location errors, i.e.  $Q$  (dependency 20) and  $Q_{av}$  (dependency 21), thus omitting the analysis of differences in location errors directly on the  $x$  and  $y$  axes of the  $x-y$  coordinate system.

## RESULTS

The results of simulation studies for guide paths no. 1-7 are presented in Figures 9–15, which show the total location errors for the GEO, TRI, and LM algorithms.

In turn, Figure 16 shows the collective localisation results of the analyzed algorithms for guide path no. 1–7. In order to qualitatively summarise the obtained localisation results, Figure 17

presents the results of quality indicators for TRI, LM and GEO for the analysed guide paths, while Figure 18 shows the average  $Q_{av}$  values for the mentioned algorithms, which were determined based on the results for guide paths no. 1–7.

The LM algorithm obtained the lowest value of the average quality index  $Q_{av}$  (21.15 m). In turn, the value obtained using TRI is approximately 1.6 times greater than the above indicator (34.28 m), and the value obtained using GEO (81.08 m) is approximately 3.8 times greater than the value obtained using LM.

## DISCUSSION

The key feature of localisation algorithms is their accuracy, which is linked to localisation errors. In connection with the above, total localisation errors were determined for all considered algorithms. Due to the variability of the total error values for individual paths and algorithms, a quality indicator was determined as the sum of total errors. It was assumed that the most accurate

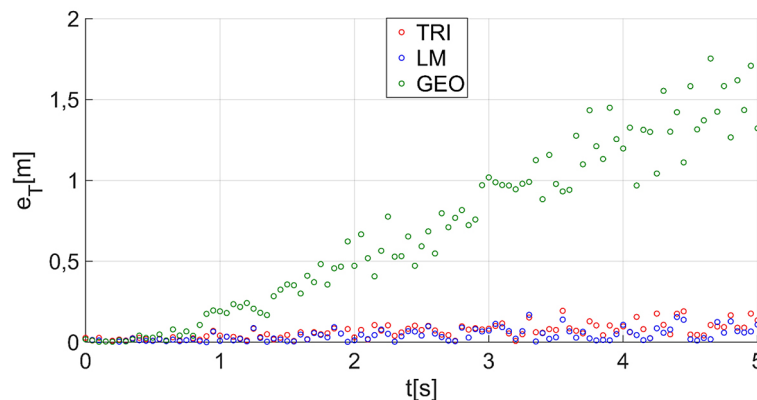


Figure 9. The course of the total location errors  $e_T(t)$  for path no. 1

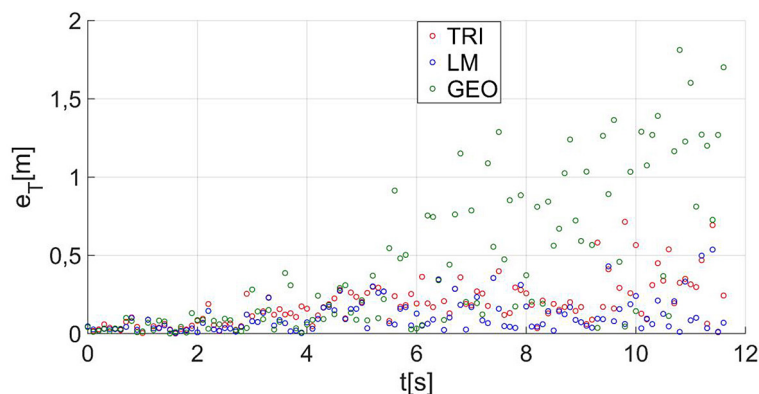


Figure 10. The course of the total location errors  $e_T(t)$  for path no. 2

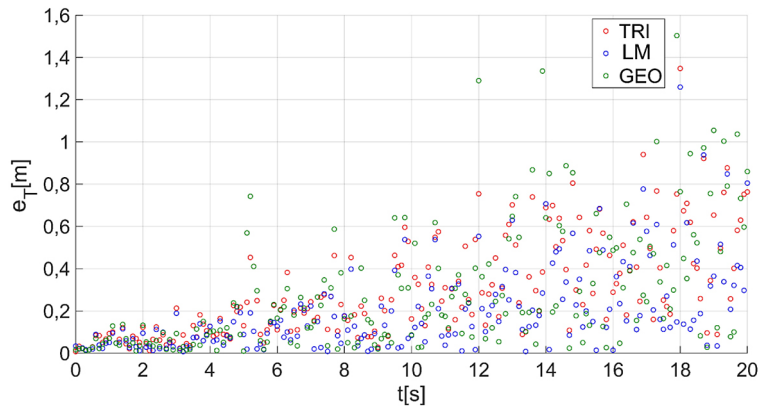


Figure 11. The course of the total location errors  $e_T(t)$  for path no. 3

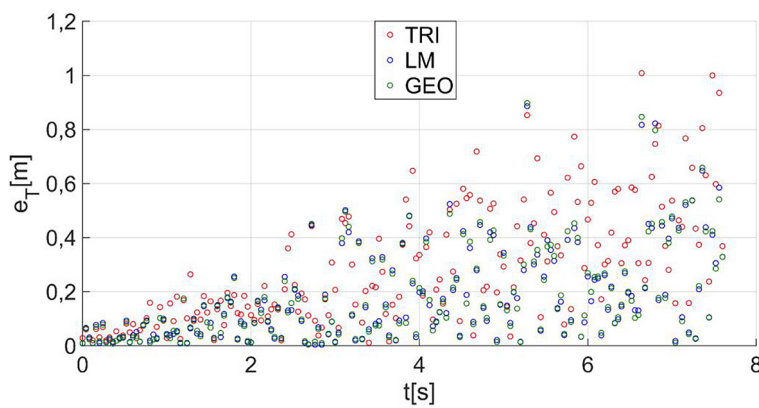


Figure 12. The course of the total location errors  $e_T(t)$  for path no. 4

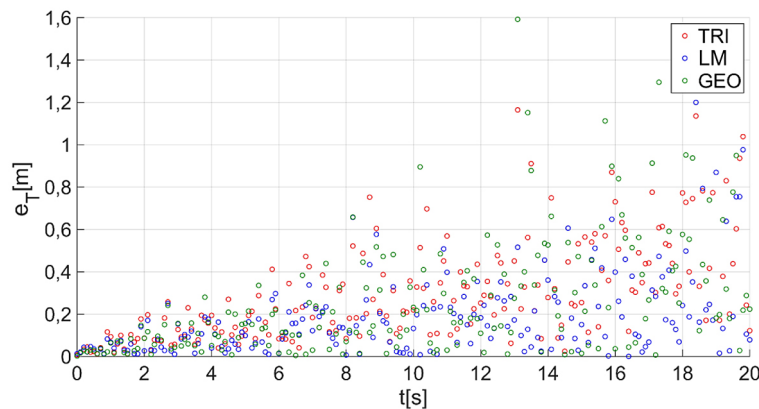


Figure 13. The course of the total location errors  $e_T(t)$  for path no. 5

algorithm should be characterised by the minimum value of errors, in the discussed case of the average quality indicator. In this context, the most accurate algorithm was LM, and the least accurate algorithm was GEO.

Figure 9–15 shows the total errors for all the analysed algorithms for paths no. 1–7. In the case of paths no. 1, 2, 6 and 7, it can be easily noticed

that the values of the total errors for the GEO algorithm are much higher than for TRI and LM. This is due to the fact that the measurement noise has the greatest impact on the solution of the quadratic equation (the basis of this algorithm) for the “extreme” paths, i.e. the ones furthest from path no. 4 (in the direction of the y-axis). The difference in error values is not as noticeable for

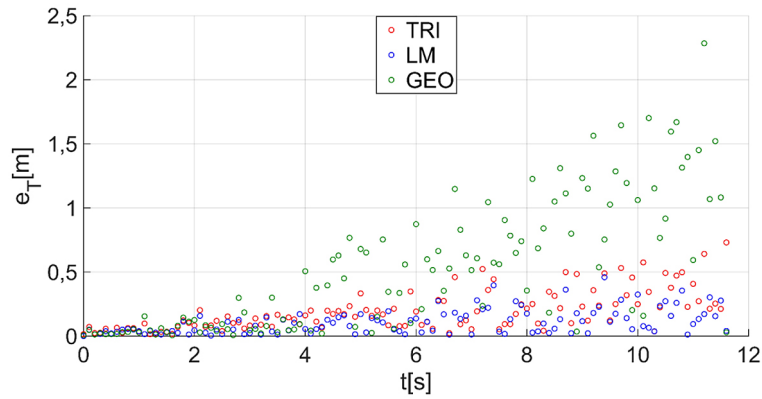


Figure 14. The course of the total location errors  $e_T(t)$  for path no. 6

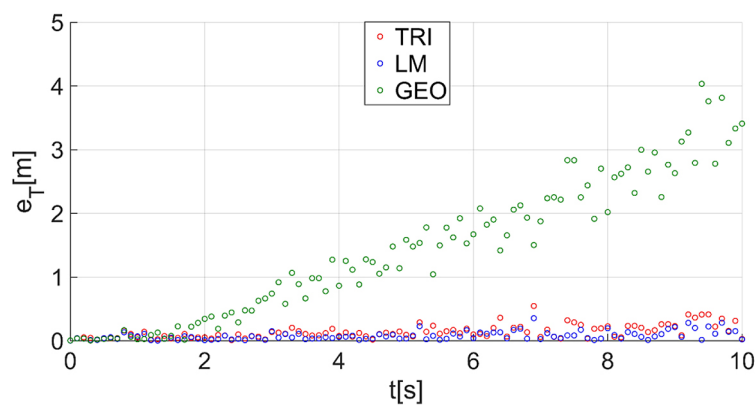


Figure 15. The course of the total location errors  $e_T(t)$  for path no. 7

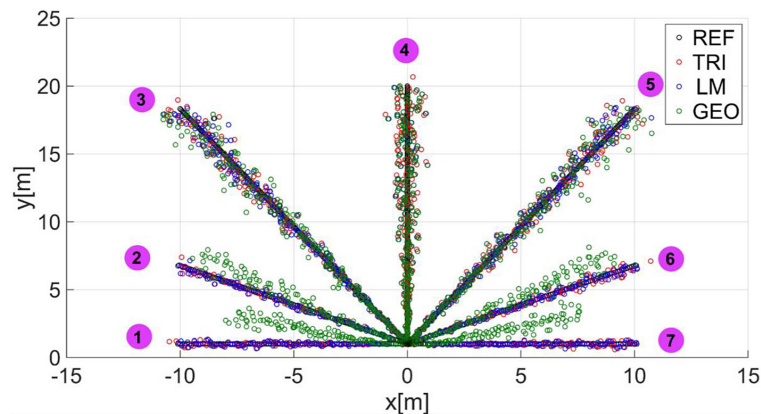


Figure 16. The results of the guide location for paths 1–7. Own elaboration based on [10]

paths no. 3, 4 and 5. The GEO method generated the largest location errors for marginal paths no. 1 and 7, while in the case of the TRI and LM methods, the largest errors occurred in the case of paths no. 3, 4 and 5. The GEO method, due to the least complex mathematical model and high susceptibility to interference, obtained the highest value of the average quality index  $Q_{av}$ .

Figure 16 presents a graphical summary of localisation results for all analyzed paths. Also in this case it can be seen that the most accurate localisation concerns the LM and TRI algorithms, for which the obtained path is consistent with the reference path. In the case of the GEO algorithm, a clear deviation towards paths no. 1, 2, 6, and 7 can be seen.

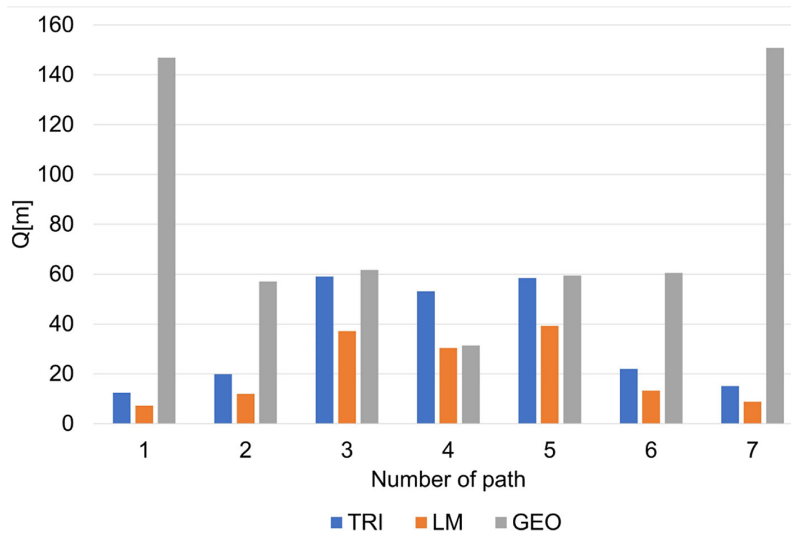


Figure 17. Results of quality indicators  $Q$  for guide paths no. 1–7. Own elaboration based on [10]

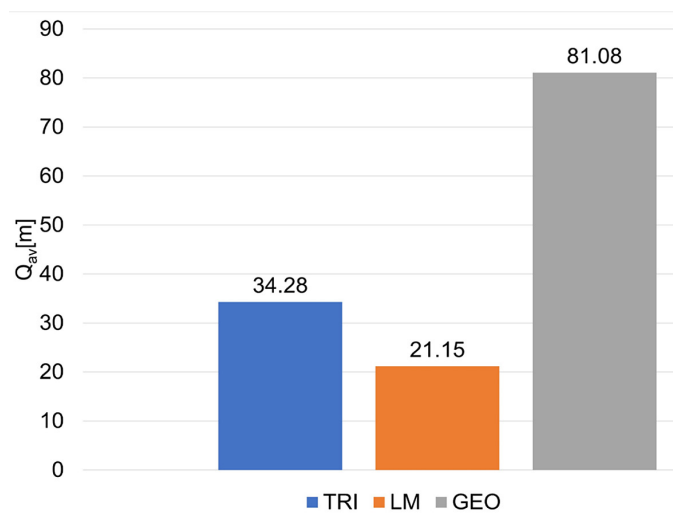


Figure 18. Results of average quality indicators  $Q_{av}$  for selected localisation algorithms. Own elaboration based on [10]

## CONCLUSIONS

The intentional disturbance introduced in the simulated distance measurements of individual anchors has a significant impact on the total location errors in the case of algorithms LM, TRI and GEO (Figures 9–16).

The TRI and LM algorithms maintain the assumed linearity of the target path (Figure 16) and are characterised by moderate total error values. The computational complexity of the optimisation methods (LM) guarantees better accuracy, but at the cost of computation time. TRI, on the other hand, has a linear mathematical model, which guarantees high speed of operation, but at the cost of accuracy. TRI is also more exposed to the occurrence of measurement noise.

The most accurate in the context of guide location among the analysed algorithms was LM, which results from the most complex mathematical model requiring iterative calculations to determine the guide location.

The large discrepancy in the obtained results (Figure 16) indicates the need to use signal filtering (for guide localisation results) in the processing of experimental data.

## Funding

This work was financed/co-financed by the Military University of Technology under research project UGB 708/2024.

## REFERENCES

1. UGV. Available online: <https://www.unmannedsystemstechnology.com/expo/unmanned-ground-vehicle-ugv-manufacturers/> (accessed on 18 April 2024).
2. Michalski K., Nowakowski M. The use of unmanned vehicles for military logistic purposes. *Zeszyty Naukowe Szkoły Głównej Gospodarstwa Wiejskiego w Warszawie. Ekonomika i Organizacja Logistyki*, 2020, 5(4), 43–57.
3. Husky. Available online: <https://clearpathrobotics.com/husky-unmanned-ground-vehicle-robot/> (accessed on 18 April 2024).
4. PROBOT. Available online: <https://robo-team.com/products/probot/> (accessed on 18 April 2024).
5. Bonadies S., Lefcourt A., Gadsden S. A. A survey of unmanned ground vehicles with applications to agricultural and environmental sensing. In: *Autonomous air and ground sensing systems for agricultural optimization and phenotyping*, 2016, 9866, 142–155, SPIE.
6. BURRO. Available online: <https://www.agriaautomation.co.nz/burro/> (accessed on 18 April 2024).
7. Hu X., Assaad R. H. The use of unmanned ground vehicles (mobile robots) and unmanned aerial vehicles (drones) in the civil infrastructure asset management sector: Applications, robotic platforms, sensors, and algorithms. *Expert Systems with Applications*, 2023, 232, 120897.
8. Taffetas S.G. *Introduction to Mobile Robot Control*, Elsevier, 2014.
9. Bartnicki A.: Wymagania dla stanowiska zdalnego sterowania pojazdem bezzałogowym w zadaniach zmniejszenia zagrożenia wywołanego niekontrolowanym uwalnianiem substancji niebezpiecznych. *Logistyka*, 2012, 3.
10. Rykała Ł. Kształtowanie systemu lokalizacji przewodnika w aspekcie wyznaczania trasy przejazdu platformy bezzałogowej. PhD Thesis. Military University of Technology, Warsaw, 2021.
11. Liu Q., Li Z., Yuan S., Zhu Y., Li X. Review on vehicle detection technology for unmanned ground vehicles. *Sensors*, 2021, 21(4), 1354.
12. Liu O., Yuan S., Li Z. A survey on sensor technologies for unmanned ground vehicles. In: *2020 3rd International Conference on Unmanned Systems (ICUS)*, 2020, 638–645, IEEE.
13. Islam MJ, Hong J, Sattar J. Person-following by autonomous robots: A categorical overview. *The International Journal of Robotics Research*. 2019, 38(14), 1581–1618.
14. Bakar M. N. A., Amran M. F. M. A study on techniques of person following robot. *International Journal of Computer Applications*, 2015, 125(13).
15. Dabbeeru M. M., Langsfeld J. D., Svec P., Gupta S. K.: Towards Energy Efficient Follow Behaviors for Unmanned Ground Vehicles Over Rugged Terrains. *ASME 2012 International Design Engineering Technical Conferences and Computers and Information in Engineering Conference*, American Society of Mechanical Engineers, 2012, 1307–1317.
16. Sadeghi-Tehran P., Andreu J., Angelov P., Zhou X.: Intelligent leader-follower behaviour for unmanned ground-based vehicles. *Journal of Automation Mobile Robotics and Intelligent Systems*, 2011, 5, 36–46.
17. Rykała Ł., Typiak A., Typiak R. Research on developing an outdoor location system based on the ultra-wideband technology. *Sensors*, 2020, 20(21), 6171.
18. Demetriou G. A. A Survey of Sensors for Localization of Unmanned Ground Vehicles (UGVs). In: *IC-AI*, 2006, 659–668.
19. Shan X., Cabani A., Chafouk H. A Survey of Vehicle Localization: Performance Analysis and Challenges, 2023, IEEE Access.
20. Mannay K., Benhadjoussef N., Machhout M., Urena J. Location and positioning systems: Performance and comparison. In: *2016 4th International Conference on Control Engineering Information Technology (CEIT)*, 2016, 1–6, IEEE.
21. Cheok K. C., Liu B., Hudus G. R., Overholt J. L., Skalny M., Smid G. E. Ultra-Wideband methods for UGV positioning: Experimental and simulation results. In: *Procs. of 2006 US Army Science Conference*, 2006.
22. Rykała Ł., Typiak A., Typiak R., Rykała M. Application of Smoothing Spline in Determining the Unmanned Ground Vehicles Route Based on Ultra-Wideband Distance Measurements. *Sensors*, 2022, 22(21), 8334.
23. Deremetz M., Lenain R., Laneurit J., Debain C., Peynot T. (2020). Autonomous Human Tracking using UWB sensors for mobile robots: An Observer-Based approach to follow the human path. In: *2020 IEEE Conference on Control Technology and Applications (CCTA)*, 2020, 372–379, IEEE.
24. Ultra Wideband technology for indoor positioning and navigation. Available online: <https://navigine.com/blog/uwb-technology-features-examples-of-application/> (accessed on 18 April 2024).
25. Mohd Sultan J., Kamaruzaman N. N., Chaudhary A. R., Yusop A., M., Manap Z., Mohd Ali D. Precision Indoor Positioning with Ultra-Wideband (UWB) Technology. *Przegląd Elektrotechniczny*, 2024, 5.
26. Chen Y., Wang J., Yang J. Exploiting anchor links for NLOS combating in UWB localization. *ACM Transactions on Sensor Networks*, 2024, 20(3), 1–22.
27. Liu C. Ultra Wide Band Technology and Indoor Precise Positioning. In: *SHS Web of Conferences*, 2022, 144, 02002, EDP Sciences.
28. Otim T., Díez L. E., Bahillo A., Lopez-Iturri P.,

- Falcone F. Effects of the body wearable sensor position on the UWB localization accuracy. *Electronics*, 2019, 8(11), 1351.
29. TREK 1000. Available online: [https://www.decawave.com/wp-content/uploads/2018/09/trek1000\\_user\\_manual.pdf](https://www.decawave.com/wp-content/uploads/2018/09/trek1000_user_manual.pdf) (accessed on 18 April 2024).
  30. Two-Way Ranging. Available online: <https://www.sewio.net/uwb-technology/two-way-ranging/> (accessed on 18 April 2024).
  31. Malon K., Łopatka J., Rykała Ł., Łopatka M. Accuracy Analysis of UWB Based Tracking System for Unmanned Ground Vehicles. 2018 New Trends in Signal Processing (NTSP), IEEE, 2018, 1–7.
  32. Long L., Wu J. Research on Indoor Fusion Positioning Based on EKF for Uwb\_Imu. *Academic Journal of Science and Technology*, 2023, 8(1), 156–160.
  33. Wang C., Han H., Wang J., Yu H., Yang D. A robust extended Kalman filter applied to ultrawideband positioning. *Mathematical Problems in Engineering*, 2020(1), 1809262.
  34. Zhou Y. An Effective Trilateration Algorithm for Mobile Robot Positioning Based on Multiple Reference Points. In: *International Design Engineering Technical Conferences and Computers and Information in Engineering Conference*, 2009, 49040, 1147–1155.
  35. Doukhnitch E., Salamah M., Ozen E. An efficient approach for trilateration in 3D positioning. *Computer communications*, 2008, 31(17), 4124–4129.
  36. Pelka M. Position Calculation with Least Squares based on Distance Measurements. Lübeck University of Applied Sciences: Technical Report, 2015, 1–3.
  37. Zhou Y. An efficient least-squares trilateration algorithm for mobile robot localization. In: *Proceedings of the 2009 IEEE/RSJ International Conference on Intelligent Robots and Systems*, 2009, 3474–3479.
  38. Guo H., Li M., Zhang X., Gao X., Liu Q. UWB indoor positioning optimization algorithm based on genetic annealing and clustering analysis. *Frontiers in Neurorobotics*, 2022, 16, 715440.
  39. Shaker S., Saade J. J., Asmar D. Person-following using fuzzy inference. In: *Proceedings of the WSEAS International Conference on Applied Computer and Applied Computational Science*, 2008.
  40. Brzezinski M., Kijek M., Gontarczyk M., Rykała Ł., Zelkowski J. Fuzzy modeling of evaluation logistic systems. In *Proceedings of the 21st International Scientific Conference Transport Means 2017*, Juodkrante, Lithuania, September 2017; Kaunas University of Technology: Kaunas, Lithuania; 377–382.
  41. Laaraiedh M., Yu L., Avrillon S., Uguen B. Comparison of hybrid localization schemes using RSSI, TOA, and TDOA. In: *17th European Wireless 2011-Sustainable Wireless Technologies*, 2011, 1–5, VDE.
  42. Kozicki B., Skrabacz A. A comparative analysis of injuries and deaths caused by road traffic accidents in Poland and selected EU countries. *Transport Problems: an International Scientific Journal*, 2024, 19(1).
  43. Kozicki B., Mitkow Sz., Jaśkiewicz P. The Use of Chernoff Faces to Depict Losses in the Number of Passengers Transported by Air in Australia. In *Proceedings of the 25th International Scientific Conference Transport Means 2021*, Juodkrante, Lithuania, October 2021; Kaunas University of Technology: Kaunas, Lithuania; 1231–1235.